



Entanglement Tsunami: Universal Scaling in Holographic Thermalization

Hong Liu* and S. Josephine Suh†

Center for Theoretical Physics, Massachusetts Institute of Technology, Cambridge, Massachusetts 02139, USA

(Received 27 June 2013; published 7 January 2014)

We consider the time evolution of entanglement entropy after a global quench in a strongly coupled holographic system, whose subsequent equilibration is described in the gravity dual by the gravitational collapse of a thin shell of matter resulting in a black hole. In the limit of large regions of entanglement, the evolution of entanglement entropy is controlled by the geometry around and inside the event horizon of the black hole, resulting in regimes of pre-local-equilibration quadratic growth (in time), post-local-equilibration linear growth, a late-time regime in which the evolution does not carry memory of the size and shape of the entangled region, and a saturation regime with critical behavior resembling those in continuous phase transitions. Collectively, these regimes suggest a picture of entanglement growth in which an “entanglement tsunami” carries entanglement inward from the boundary. We also make a conjecture on the maximal rate of entanglement growth in relativistic systems.

DOI: 10.1103/PhysRevLett.112.011601

PACS numbers: 11.25.Tq, 03.67.Bg, 04.70.Dy, 05.70.Ln

Introduction.—Understanding whether and how a quantum many-body system equilibrates is a question that permeates many areas of physics. One could also view equilibration as a useful setting in which to study the generation of entanglement between subsystems.

In this Letter, we consider the evolution of entanglement entropy after a global quench in a strongly coupled gapless system with a gravity dual, extending earlier results in [1–10]. We find that the entanglement entropy exhibits a variety of scaling behaviors which lead to a strikingly simple geometric picture for entanglement growth. Via holographic duality, equilibration from a generic initial many-body state maps to the formation of a black hole in the bulk, connecting questions about equilibration to those about black holes.

Setup.—At $t = 0$, we turn on external sources for an interval δt in a d -dimensional boundary system, creating a spatially homogeneous and isotropic excited state with nonzero energy density, which subsequently equilibrates. We work in the quench limit, taking the sourcing interval δt to zero. On the gravity side, such a quench is described by an infinitesimally thin shell of matter which collapses to form a black hole, and can be modeled by an anti-de Sitter (AdS)-Vaidya metric of the form

$$ds^2 = \frac{L^2}{z^2} [-f(v, z)dv^2 - 2dv dz + d\vec{x}^2], \quad (1)$$

with $f(v, z) = 1 - \theta(v)g(z)$. Our results do not depend on the matter fields making up the shell; in the classical gravity regime we are working with, which translates to the large N and strong coupling limit of the boundary theory, the entanglement entropy is sensitive only to the metric of the collapsing geometry.

For $v < 0$, the metric (1) is that of pure AdS corresponding to the vacuum state before the quench, and for $v > 0$ it is that of a black hole,

$$ds^2 = \frac{L^2}{z^2} [-h(z)dv^2 - 2dv dz + d\vec{x}^2], \quad (2)$$

where we can view $h(z) \equiv 1 - g(z)$ as parametrizing final equilibrium states. Seeking behavior “universal” to equilibrium states, we consider a general $h(z)$ which (i) has a simple zero at the event horizon $z = z_h$, (ii) can be expanded as $h(z) = 1 - Mz^d + \dots$ near the boundary $z = 0$, (iii) is positive and monotonically decreasing as a function of z for $z < z_h$, as required by the IR-UV connection, and (iv) is such that the metric (2) satisfies the null energy condition. We assume that any such $h(z)$ can be realized by a suitable arrangement of matter fields. Representative examples of such $h(z)$ include $g(z) = Mz^d$ (AdS-Schwarzschild) and $g(z) = Mz^d - Q^2 z^{2d-2}$ [AdS-Reissner-Nordström (RN)] which corresponds to an equilibrium state with nonzero charge density proportional to Q . The temperature, energy, and entropy density of the equilibrium state corresponding to (2) are given by $T = |h'(z_h)|/4\pi$, $\mathcal{E} = (L^{d-1}/8\pi G_N)((d-1)/2)M$, and $s_{\text{eq}} = (L^{d-1}/z_h^{d-1})(1/4G_N)$, where G_N is Newton’s constant in the bulk.

Now let us consider a spatial region in the boundary theory bounded by a smooth surface Σ . The entanglement entropy of this region can be obtained as $S_\Sigma(t) = \mathcal{A}_\Sigma/4G_N$, where \mathcal{A}_Σ is the area of a $(d-1)$ -dimensional extremal surface in the bulk ending at Σ on the boundary [2,11]. We define the size R of Σ to be the height of its future domain of dependence [12].

Denote by $\Delta S_\Sigma(t)$ the difference of the entanglement entropy with that in the vacuum. After the quench, $\Delta S_\Sigma(t)$ evolves from 0 at $t = 0$ to the equilibrium value

$\Delta S_{\Sigma}^{(\text{eq})} = s_{\text{eq}} V_{\Sigma}$ (for sufficiently large R), where V_{Σ} is the volume of the region bounded by Σ . Taking $\delta t = 0$, $S_{\Sigma}(t)$ saturates at $S_{\Sigma}^{(\text{eq})}$ at a sharp saturation time t_s and remains constant afterward [1,3–5].

To describe our results we introduce a “local equilibrium scale” ℓ_{eq} , which is a time scale at which the system has ceased production of thermodynamic entropy. For an equilibration process described by (1), we identify it as $\ell_{\text{eq}} \sim z_h \sim (1/s_{\text{eq}})^{1/(d-1)}$. For Schwarzschild $h(z)$, $\ell_{\text{eq}} \sim 1/T$, while for RN $h(z)$, ℓ_{eq} can be much smaller than $1/T$ when Q is large. Importantly, at times of order ℓ_{eq} , local thermodynamics applies at scales comparable to or smaller than ℓ_{eq} , but the entanglement entropy $S_{\Sigma}(t)$ and other nonlocal observables defined over large distances remain far from their equilibrium values, for $R \gg \ell_{\text{eq}}$.

We are interested in probing quantum entanglement at macroscopic scales, and take $R \gg \ell_{\text{eq}}$. On the gravity side, there is an important distinction between extremal surfaces for $R \lesssim \ell_{\text{eq}}$ and $R \gg \ell_{\text{eq}}$. If $R \lesssim \ell_{\text{eq}}$, the evolution lasts a time of order $t \lesssim \ell_{\text{eq}}$ and extremal surfaces stay outside the horizon during the entire evolution. If $R \gg \ell_{\text{eq}}$, the evolution is controlled by the geometry around and inside the horizon for $t \gtrsim \ell_{\text{eq}}$. Turning this around, we can use entanglement entropy (and other nonlocal observables such as Wilson loops and correlation functions) to probe the geometry behind the horizon of a collapsing black hole. This is in contrast to static cases where extremal surfaces always stay outside the horizon [12].

Results.—To find $S_{\Sigma}(t)$, one proceeds to solve the equations for an extremal surface in (1) with given boundary conditions and evaluate its area. By identifying various geometric regimes for the bulk extremal surface, we can extract the analytic behavior of $S_{\Sigma}(t)$ during corresponding stages of time evolution. An important observation is of the existence of a family of “critical extremal surfaces” which lie inside the horizon and separate extremal surfaces that reach the boundary from those which fall to the black hole singularity. In particular, for $R, t \gg \ell_{\text{eq}}$, the leading behavior of the entanglement entropy can be obtained from the geometry of such critical extremal surfaces. Here we discuss our main results and their physical implications, leaving a detailed technical exposition to elsewhere [13].

(i) Pre-local-equilibration growth: For $t \ll \ell_{\text{eq}}$, the entanglement entropy grows as

$$\Delta S_{\Sigma}(t) = \frac{\pi}{d-1} \mathcal{E} A_{\Sigma} t^2 + \dots, \quad (3)$$

where \mathcal{E} is the energy density and A_{Σ} is the area of Σ . This result is independent of the shape of Σ , spacetime dimension d , and form of $h(z)$. For $d = 2$ the quadratic time dependence was also obtained in [14], and is implicit in [5,6].

(ii) Post-local-equilibration linear growth: For $R \gg t \gg \ell_{\text{eq}}$, we find a universal linear growth

$$\Delta S_{\Sigma}(t) = v_E s_{\text{eq}} A_{\Sigma} t + \dots, \quad (4)$$

where v_E is a dimensionless number which is independent of the shape of Σ , but does depend on the final equilibrium state. It is given by

$$v_E = (z_h/z_m)^{d-1} \sqrt{-h(z_m)}, \quad (5)$$

where z_m is a minimum of $h(z)/z^{2(d-1)}$ and lies inside the horizon. For Schwarzschild $h(z)$,

$$v_E^{(S)} = \frac{(\eta-1)^{(1/2)(\eta-1)}}{\eta^{(1/2)\eta}}, \quad \eta \equiv \frac{2(d-1)}{d}, \quad (6)$$

while for RN $h(z)$,

$$v_E^{(\text{RN})} = \sqrt{\frac{1}{\eta-1} \left[\left(1 - \frac{u}{\eta}\right)^{\eta} - (1-u) \right]^{1/2}}, \quad (7)$$

where $u \equiv 4\pi z_h T/d$ decreases monotonically from 1 to 0 as Q increases from 0 to ∞ , at fixed T . Note that $v_E^{(S)} = 1$ for $d = 2$ and monotonically decreases with d , while $v_E^{(\text{RN})}$ monotonically increases with u —turning on a nonzero charge density slows down the evolution. Equation (4) generalizes previous observations of linear growth for $d = 2$ [1,3]. With a different bulk setup, the linear growth (4) as well as (5) and (6) were obtained recently in [15].

(iii) Saturation: The evolution beyond the linear regime depends on the shape, spacetime dimension d , and the final equilibrium state. We focus on the most symmetric shapes, with Σ being a sphere or strip and R being the radius or half-width, respectively.

For a strip in $d \geq 3$, the linear behavior (4) persists all the way to saturation which occurs at time

$$t_{s,\text{strip}}(R) = \frac{S_{\text{strip}}^{(\text{eq})}}{v_E s_{\text{eq}} A_{\text{strip}}} + \dots = \frac{R}{v_E} + O(R^0), \quad (8)$$

when the bulk extremal surface jumps discontinuously. This is analogous to a first-order phase transition with the first derivative of $S_{\Sigma}(t)$ being discontinuous at t_s . [16] Similar behavior occurs for a sphere in $d = 3$ when the final state is given by a RN black hole with sufficiently large Q [17].

For a sphere in $d \geq 4$ and any $h(z)$, the approach to saturation resembles that of a continuous phase transition and is characterized by a nontrivial scaling exponent

$$S_{\text{sphere}}(R, t) - S_{\text{sphere}}^{(\text{eq})}(R) \propto -(t_s - t)^{\gamma}, \quad \gamma = \frac{d+1}{2}, \quad (9)$$

where $t_s - t \ll \ell_{\text{eq}}$. The same exponent also applies in $d = 2$ for a Banados-Zanelli-Teitelboim (BTZ) black hole

as was recently found in [14]. In $d = 3$, if saturation is continuous, we find $S_{\text{sphere}}(t, R) - S_{\text{sphere}}^{(\text{eq})}(R) \propto (t_s - t)^2 \times \log(t_s - t)$, with the logarithmic scaling barely avoiding the “mean-field” exponent $\gamma = 2$. Meanwhile, the saturation time for a sphere, again in cases where saturation is continuous, is

$$t_s(R) = \frac{1}{c_E} R - \frac{d-2}{4\pi T} \log R + O(R^0), \quad (10)$$

with $c_E = \sqrt{\frac{z_h |h'(z_h)|}{2(d-1)}} = \sqrt{\frac{2\pi z_h T}{d-1}}$ being a dimensionless number which for Schwarzschild and RN $h(z)$ becomes $c_E^{(\text{S})} = 1/\sqrt{\eta}$ and $c_E^{(\text{RN})} = \sqrt{u/\eta} \leq c_E^{(\text{S})}$. Note that for $d = 2$, $c_E = 1$ and the logarithmic term in (10) disappears, which gives the results in [1,3,5].

(iv) Late-time memory loss: For a sphere, there is an additional scaling regime $t_s \gg t_s - t \gg \ell_{\text{eq}}$ in which $S(R, t)$ only depends on $t_s(R) - t$, and not on t and R separately [18]. There,

$$S(R, t) - S_{\text{eq}}(R) = -s_{\text{eq}} \lambda[t_s(R) - t], \quad (11)$$

where λ is some function that depends on $h(z)$ and which we have only determined for $d = 2$ and BTZ $h(z)$, $\lambda(y) = \{y + (1/2\pi T) \log[\sin \chi^{-1}(2\pi T y)]\}$, with $y = R - t$ and $\chi(\varphi) = (\cot(\varphi/2) - 1) + \log \tan(\varphi/2)$. Note that $\lambda(y)$ interpolates between the linear (4) and critical (9) behavior for, respectively, large and small $2\pi T y$. Bulk extremal surfaces in this late-time regime trace the horizon. For $d = 2$, the equivalent of (11) was first observed in [3,6].

Physical interpretation.—Equation (4) can be rewritten

$$\Delta S_{\Sigma}(t) = s_{\text{eq}}(V_{\Sigma} - V_{\Sigma - v_E t}) + \dots, \quad (12)$$

where $V_{\Sigma - v_E t}$ denotes the volume of the region bounded by a surface obtained from Σ by moving every point inward by a distance $v_E t$ (see Fig. 1). This suggests a simple geometric picture of entanglement growth: a wave with a sharp wave front propagates inward from Σ , such that the region it has covered is entangled with the region outside Σ , while the region yet to be covered is not. We call this wave an

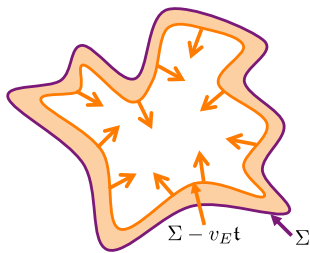


FIG. 1 (color online). The growth of entanglement entropy can be visualized as occurring via an “entanglement tsunami” with a sharp wave front carrying entanglement inward from Σ .

“entanglement tsunami.” In this picture, saturation occurs when the tsunami covers the full region.

The tsunami picture suggests that the evolution of entanglement is local. This is natural as the time evolution in our system occurs via a local Hamiltonian which couples directly only to the degrees of freedom near Σ , and entanglement has to build up from Σ . When R is large, the curvature of Σ is negligible at early times and there is no “interaction” between parts of the tsunami, which explains the shape independence and area law of (3) and (4). As the tsunami advances inward, curvature effects become important and it propagates nonlinearly due to interaction between its parts, resulting in shape-dependent saturation.

For a strip in $d \geq 3$, Eq. (8) suggests tsunamis from two boundaries propagate freely until they meet, causing discontinuous saturation. For a sphere in $d \geq 3$, $1 > c_E > v_E$, where the latter inequality may be understood geometrically from the fact that the volume of an annulus region of unit width becomes smaller as the tsunami advances inward. The former inequality, along with the presence of the logarithm in (10) and the nontrivial exponent γ in (9), may be considered a consequence of interactions between parts of the tsunami. In contrast, in $d = 2$, where Σ consists of two points, $c_E = v_E = 1$.

Finally, given $S_{\text{eq}}(R) = V_{\Sigma} s_{\text{eq}}$, one can interpret λ in (11) as the volume which has not yet been entangled, and (11) as implying that that volume only depends on $t_s - t$ and not on R and t separately. In other words, the size R has been “forgotten” at late times of evolution. Note that with (11) valid for $t_s \gg t_s - t \gg \ell_{\text{eq}}$, such memory loss can happen long before saturation. It is tempting to speculate that for a generic surface Σ , in the limit of large R , memory of both the size and shape of Σ could be lost during late times of evolution. This would also imply that the critical behavior (9) near saturation applies to a wide class of compact surfaces and not just the sphere.

The linear growth regime (4) sets in only after local equilibration has been achieved. This explains the appearance of equilibrium entropy density s_{eq} in the prefactor. In contrast, pre-local-equilibration quadratic growth (3) is proportional to the energy density \mathcal{E} . Indeed, at very early times before the system has equilibrated locally, the only macroscopic data characterizing the initial state is the energy density. Conversely, if we stipulate that before local equilibration $S_{\Sigma}(t)$ should be proportional to A_{Σ} and \mathcal{E} , the quadratic time dependence in (3) follows from dimensional analysis. Similarly, if we require that after local equilibration $S_{\Sigma}(t)$ is proportional to A_{Σ} and s_{eq} , linearity in time follows.

In [1], a model of entanglement growth from free-streaming “quasiparticles” was proposed which gave a nice explanation for the linear growth and saturation of entanglement entropy in $d = 2$. In particular, $v_E = c_E = 1$ followed from quasiparticles propagating at the speed of light. In a companion paper with Mezei [19],

we generalize the free-streaming model to higher dimensions and again find that at early times there is linear growth as in (4) with s_{eq} interpreted as giving a measure for quasiparticle density. The quasiparticle model can also be generalized to capture the pre-local-equilibration quadratic growth (3), if one takes into account that during local equilibration the quasiparticle density gradually builds up [19]. Since the quasiparticles can travel in different directions in $d \geq 3$, although their individual speed is set to 1, the speed of the entanglement tsunami is smaller than 1, and is given by [19]

$$v_E^{(\text{streaming})} = \frac{\Gamma((d-1)/2)}{\sqrt{\pi}\Gamma(d/2)} < v_E^{(S)} < 1. \quad (13)$$

Notably, this speed is smaller than even the Schwarzschild value (6)—in strongly coupled systems, the propagation of entanglement entropy is faster than that from free-streaming particles moving at the speed of light. Recall that a hallmark of a strongly coupled system with a gravity dual is the absence of a quasiparticle description. Thus, while the quasiparticle model appears to capture linear growth, it is likely missing some important elements present in a holographic system, e.g., multibody entanglement. Also, note that in the quasiparticle model, $t_s = R$ for a sphere, implying faster saturation than in (10), as $c_E < 1$ for $d \geq 3$.

Generality.—Since the entanglement tsunami picture followed from evolution under a local Hamiltonian, we expect it to apply to more general equilibration processes for which the initial state is not necessarily homogeneous or isotropic, and even to systems without translation invariance. With nonzero δt , the wave front will develop a finite spread, but the entanglement tsunami picture may apply as long as one considers entangled regions much larger than δt . If δt is comparable to or larger than ℓ_{eq} , the pre-local-equilibration and saturation regimes can no longer be sharply defined, but post-local-equilibration linear growth should still exist, as could late-time memory loss. An important feature of the linear growth (4) is that the tsunami speed v_E characterizes properties of the equilibrium state, as it is solely determined by the metric of the black hole. This again highlights the local nature of entanglement propagation. At corresponding times, locally, the system has already achieved equilibrium, although for large regions nonlocal observables such as entanglement entropy remain far from their equilibrium values. Thus, v_E should be independent of the nature of the initial state, including whether it was isotropic or homogeneous. Finally, that the early growth (3) is proportional to the energy density is consistent with other recent studies of the entanglement entropy of excited states [20–23].

Maximal entanglement rate?—To compare the growth of entanglement entropy between different systems, we introduce a dimensionless rate of growth

$$\mathfrak{R}_\Sigma(\mathbf{t}) \equiv \frac{1}{s_{\text{eq}} A_\Sigma} \frac{dS_\Sigma}{dt}. \quad (14)$$

In the linear regime, \mathfrak{R}_Σ is a constant given by v_E , while in the pre-local-equilibration regime $\mathbf{t} \ll \ell_{\text{eq}}$ in which (3) $\mathfrak{R}_\Sigma(\mathbf{t}) = (2\pi/d - 1)((\mathcal{E}\mathbf{t})/s_{\text{eq}})$ grows linearly with time.

In a relativistic system, v_E , and more generally $\mathfrak{R}_\Sigma(\mathbf{t})$, should be constrained by causality, although relating them directly to the speed of light appears difficult except in the quasiparticle-type model mentioned earlier. We have examined v_E for known black hole solutions and other $h(z)$ satisfying properties listed below (2) and find support that

$$v_E \leq v_E^{(S)} = \frac{(\eta - 1)^{(1/2)(\eta-1)}}{\eta^{(1/2)\eta}}. \quad (15)$$

Note that $v_E^{(S)} = 0.687, 0.620$ for $d = 3, 4$. The fact that Eq. (2) satisfies the null energy condition appears to be important for the validity of the above inequality. There are reasons to suspect that the Schwarzschild value (6) may indeed be special. The gravity limit corresponds to the infinite coupling limit of the gapless boundary Hamiltonian, in which the generation of entanglement should be most efficient. Also, one expects that, in the bulk, turning on matter fields (satisfying the null energy condition) will slow down thermalization, and that, similarly, in the boundary theory, turning on conserved quantities such as charge density will decrease the efficiency of equilibration processes. Given (13), it is tempting to conjecture that (15) applies to all relativistic systems for which a linear growth regime exist.

Turning to \mathfrak{R}_Σ , in explicit examples we find that after local equilibration (i.e., after linear growth has set in), it monotonically decreases with time. This appears natural from the tsunami picture—after the linear growth regime, interactions between parts of the tsunami are likely to slow it down. Thus, we speculate that after local equilibration,

$$\mathfrak{R}_\Sigma(\mathbf{t}) \leq v_E^{(S)}. \quad (16)$$

Before local equilibration, however, \mathfrak{R}_Σ is sensitive to the initial state, and, in particular, for RN $h(z)$ with Σ a sphere or strip, we find it can exceed $v_E^{(S)}$ near ℓ_{eq} . Also, for a highly anisotropic initial state, \mathfrak{R}_Σ could for a certain period of time resemble that of a $(1+1)$ -dimensional system for which it can reach 1. Thus, we speculate that before local equilibration,

$$\mathfrak{R}_\Sigma(\mathbf{t}) \leq 1. \quad (17)$$

Finally, the inequalities (15)–(17) are reminiscent of and can be considered as generalizations to continuum systems of the small incremental entangling conjecture for ancilla-assisted entanglement rates in a spin system [24], recently proved in [25]. Also, it would be interesting to formulate an

effective theory for the propagation of an entanglement tsunami in a general equilibration process. This would be similar in spirit to recent efforts in [26] to derive equations of motion for entanglement entropy from Einstein equations.

We thank Márk Mezei for many discussions, and also A. Adams, H. Casini, T. Faulkner, A. Harrow, T. Hartman, M. Headrick, V. Hubeny, L. Huijse, S.-S. Lee, J. Maldacena, R. Myers, S. Pufu, M. Rangamani, O. Saremi, D. T. Son, J. Sonner, B. Swingle, T. Takayanagi, E. Tonni, and J. Zaenen. Work was supported in part by funds provided by the U.S. Department of Energy (DOE) under Cooperative Research Agreement No. DE-FG0205ER41360 and the Simons Foundation.

*hong_liu@mit.edu

†jsuh@mit.edu

- [1] P. Calabrese and J. L. Cardy, *J. Stat. Mech.* (2005) P04010.
- [2] V. E. Hubeny, M. Rangamani, and T. Takayanagi, *J. High Energy Phys.* **07** (2007) 062.
- [3] J. Abajo-Arastia, J. Aparicio, and E. Lopez, *J. High Energy Phys.* **11** (2010) 149.
- [4] T. Albash and C. V. Johnson, *New J. Phys.* **13**, 045017 (2011).
- [5] V. Balasubramanian, A. Bernamonti, J. de Boer, N. Copland, B. Craps, E. Keski-Vakkuri, B. Müller, A. Schäfer, M. Shigemori, and W. Staessens, *Phys. Rev. Lett.* **106**, 191601 (2011); *Phys. Rev. D* **84**, 026010 (2011).
- [6] J. Aparicio and E. Lopez, *J. High Energy Phys.* **12** (2011) 082.
- [7] D. Galante and M. Schvellinger, *J. High Energy Phys.* **07** (2012) 096.
- [8] E. Caceres and A. Kundu, *J. High Energy Phys.* **09** (2012) 055.
- [9] W. Baron, D. Galante, and M. Schvellinger, *J. High Energy Phys.* **03** (2013) 070.
- [10] I. Aref'eva, A. Bagrov, and A. S. Koshelev, arXiv:1305.3267.
- [11] S. Ryu and T. Takayanagi, *Phys. Rev. Lett.* **96**, 181602 (2006); *J. High Energy Phys.* **08** (2006) 045.
- [12] V. E. Hubeny, *J. High Energy Phys.* **07** (2012) 093.
- [13] H. Liu and J. Suh arXiv:1311.1200.
- [14] V. E. Hubeny, M. Rangamani, and E. Tonni, *J. High Energy Phys.* **05** (2013) 136.
- [15] T. Hartman and J. Maldacena, *J. High Energy Phys.* **05** (2013) 014.
- [16] With a RN black hole, at fixed Q and sufficiently large R , the linear regime does not appear to extend all the way to saturation.
- [17] The discontinuous saturation for a strip and for a sphere in $d = 3$ for a RN black hole with a sufficiently large Q was first observed in [4]; see also Ref. [5].
- [18] The expression below may not apply in $d = 3$, where we do not yet have a clean result.
- [19] H. Liu, M. Mezei, and J. Suh (to be published).
- [20] D. D. Blanco, H. Casinia, L.-Y. Hung, and R. C. Myers, *J. High Energy Phys.* **08** (2013) 060.
- [21] J. Bhattacharya, M. Nozaki, T. Takayanagi, and T. Ugajin, *Phys. Rev. Lett.* **110**, 091602 (2013).
- [22] D. Allahbakhshi, M. Alishahiha, and A. Naseh, *J. High Energy Phys.* **08** (2013) 102.
- [23] G. Wong, I. Klich, L. A. P. Zayas, and D. Vaman, arXiv:1305.3291.
- [24] S. Bravyi, *Phys. Rev. A* **76**, 052319 (2007).
- [25] K. Van Acoleyen, M. Marien, and F. Verstraete, *Phys. Rev. Lett.* **111**, 170501 (2013).
- [26] M. Nozaki, T. Numasawa, A. Prudenziati, and T. Takayanagi, *Phys. Rev. D* **88**, 026012 (2013).